Finding finite-time invariant manifolds in two-dimensional velocity fields

G. Haller[a)]
Division of Applied Mathematics, Lefschetz Center for Dynamical Systems, Brown University, Providence, Rhode Island 02912

(Received 9 July 1999; accepted for publication 18 September 1999)

For two-dimensional velocity fields defined on finite time intervals, we derive an analytic condition that can be used to determine numerically the location of *uniformly hyperbolic* trajectories. The conditions of our main theorem will be satisfied for typical velocity fields in fluid dynamics where the deformation rate of coherent structures is slower than individual particle speeds. We also propose and test a simple numerical algorithm that isolates uniformly finite-time hyperbolic sets in such velocity fields. Uniformly hyperbolic sets serve as the key building blocks of Lagrangian mixing geometry in applications. © *2000 American Institute of Physics.* [S1054-1500(00)00501-2]

Typical time-dependent velocity fields in fluid mechanics are well-known to exhibit intense mixing of particles. For special time dependences, such as periodic, quasiperiodic, or adiabatic, dynamical systems theory has been successful in locating the geometric structures, stable and unstable manifolds, that are responsible for global mixing. At the same time, there has been no systematic tool to extract similar geometric structures for general fluid flows given for finite times. In this paper we give analytic results that can be used to identify the most important building blocks of mixing: Uniformly finite-time hyperbolic trajectories and their local stable and unstable manifolds. The results apply to any numerically or experimentally generated two-dimensional velocity field and do not assume special features of the flow (e.g., incompressibility or the presence of stagnation points).

I. INTRODUCTION

Hyperbolic or finite-time hyperbolic invariant sets are well known to act as organizing centers for mixing and transport in dynamical systems. While the vector fields associated with near-integrable, adiabatic, or relatively slow flows do provide clues about the location of their hyperbolic sets, the detection of such sets in general time-dependent flows still presents a great challenge.

Traditionally finite-time (or local) Lyapunov exponents have been employed to pinpoint hyperbolic behavior in time-dependent velocity fields. This typically involves the numerical solution of the variational equation associated with a trajectory of interest which is then used to obtain a finite-time approximation for the (infinite-time) Lyapunov exponents. Such an estimation of Lyapunov exponents requires great care and a thorough understanding of all the errors involved (see Abarbanel[1]). The resulting distribution of exponents is typically a fuzzy set, which approximates the set of all stable and unstable manifolds present in the flow. Such a picture provides a first step in the study of hyperbolic behavior in the flow, even though its building blocks are typically difficult to isolate.

The identification of regions that behave like hyperbolic sets (isolating neighborhoods) are in principle also possible using topological methods. A step in this direction has been taken by Mischaikow *et al.*,[11] who established numerical methods for the topological detection of chaotic invariant sets in experimental data sets.

An analytic result on the location of finite-time hyperbolic trajectories in velocity fields of the form

$$\dot{x}=u(x,t), \quad x\in\mathbb{R}^2, \quad tt[t_0,t_1],$$

can be found in Haller and Poje,[6] where time-dependent stagnation points of the velocity field were considered as first approximations for finite-time hyperbolic trajectories. Under a set of conditions, these stagnation points do imply the existence of nearby hyperbolic solutions. The method has been very efficient in creating mathematically rigorous mixing templates in eddy–jet interaction problems (see Haller and Poje[6] and Poje and Haller[12]). The limitation of this approach is its heavy reliance on the existence of stagnation points. In other words, only hyperbolic orbits with velocities very close to the velocity of the reference frame can be detected in this fashion.

A statistical approach to locating Lagrangian coherent structures is suggested by Mezić and Wiggins,[9] who compute average velocities for a grid of initial conditions for finite times. The resulting patchiness plots reveal regions of initial conditions with similar finite-time statistics. As shown through examples in Poje *et al.*,[13] on certain time intervals the boundaries of such regions approximate finite-time invariant manifolds. Thus, patchiness plots offer a type of ''edge detection'' that is a useful first step in the exploration of the global flow geometry.

An alternative numerical method for the global detection of hyperbolic structures in two-dimensional velocity fields has been proposed recently by Bowman.[2,3] His *finite strain map* technique approximates stable manifolds by finding the local maxima of the function

a)Electronic mail: haller@cfm.brown.edu

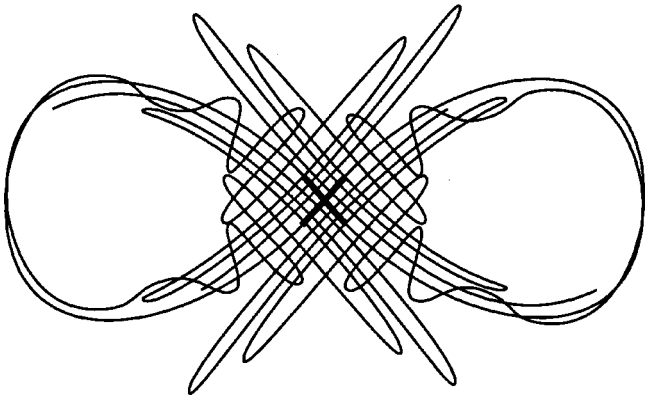

FIG. 1. Mixing geometry on a Poincaré section of the Duffing oscillator with small periodic forcing.

$$s_T(x_0) = \max_{y \in G_{x_0}} \frac{|x(T;x_0) - x(T;y)|}{|x_0 - y|},$$

where $x(t,x_0)$ denotes a solution at time $t \in [t_0, t_0+T]$ with initial condition x_0, and G_{x_0} denotes the set of nearest neighbors of the point x_0 on the grid of initial conditions. This method avoids solving variational equations and gives good approximations for global stable manifolds in several test cases. At the same time, since it effectively detects local extrema of strain, it does not necessarily imply the existence of nearby hyperbolic sets, as simple examples show. In addition, the detection of invariant manifolds will depend on the optimal choice of T which is not known *a priori*. Nevertheless, for typical mixing geometries and for appropriately chosen T regimes, the algorithm provides a useful template for global invariant manifolds.

A. Building blocks of a mixing template

It is important to realize that in order to understand the global geometry of mixing, one only needs a ''sharp'' template of the most influential finite-time hyperbolic sets. More concretely, finite-time Lyapunov exponents and finite strain maps approximate the set of all global stable and unstable manifolds that could be more accurately reproduced numerically if one knew the exact location of some organizing orbits with ''strong'' or, *uniform*, hyperbolicity. Locating the organizing centers of a mixing template is in fact essential since a convoluted set of global stable and unstable manifolds is of no immediate help if one wants to understand interaction among various regions or quantify mixing rates.

As an example, consider the Poincaré map of the ordinary Duffing equation with small forcing. The mixing geometry in this problem is completely governed by the stable and unstable manifolds of the unique uniformly hyperbolic fixed point near the origin (see Fig. 1). Therefore, instead of obtaining fuzzy global approximations for these manifolds by using any of the methods described above, one could focus on obtaining a good approximation of the local stable and unstable manifolds shown in bold in the figure. Once these sets are found, one can simply iterate the global stable and unstable manifolds until their first few intersections are found. In this fashion, a clear picture of mixing emerges which is not obstructed by the tangling of global stable and unstable manifolds.

The above example is special because of its periodic time dependence. In the general aperiodic and finite-time case, Poincaré maps are not available, and hence it is even more important to have a clear template of the ''cores'' of the mixing geometry. In addition, one would like to know exactly what one finds; when it comes to clarifying the details in mixing in a given problem, it is desirable to have an algorithm with a strong mathematical foundation. In such a case one can exclude the possibility that the results are only due to some finite-time numerical anomaly. Finally, one ideally wants to use an algorithm which is not sensitive to the choice of the time interval and the location of stable and unstable manifolds become clearer as time increases.

B. Main results

In this paper we prove an analytic result that can be used to locate uniformly finite-time hyperbolic sets and their locals stable and unstable manifolds in two-dimensional time-dependent velocity fields. Our main theorem will apply to typical oceanic or atmospheric flows where the deformation rate of coherent structures is slower than typical particle speeds. The conditions of the theorem are formulated in terms of the eigenvectors and eigenvalues of the Jacobian of the vector field along trajectories.

Based on our main theorem, we also propose a simple numerical scheme that gives a first approximation for uniformly hyperbolic structures in two-dimensional fluid flows. In particular, such structures and their local stable manifolds will appear as local maxima of the scalar field

$$d_T(x_0) = \max_{t \in [t_0, t_0+T]} \{t \,|\, \det D_x u(x(\tau;x_0),\tau) < 0, \quad t_0 \leqslant \tau < t\}.$$

In words, $d_T(x_0)$ is the maximal time for the initial condition that it spends in a domain where the determinant of the Jacobian of the velocity field is strictly negative. If $\det D_x u(x(t_0;x_0),t_0) \geqslant 0$, then by definition $d_T(x_0) = 0$ for any T.

An advantage of this algorithm is that a contour plot of d_T produces sharper and sharper images of local stable manifolds and hence is not sensitive to the choice of T. Another important computational advantage is that one does not have to iterate the whole grid of initial conditions for all times up to T. In fact, the number of particles to follow decays rapidly as for most of them $\det D_x u(t(\tau;x_0),t)$ turns positive at some point, and hence $d_T(x_0)$ is obtained without increasing the time of iteration to T. The particles that exhibit $\det D_x u(x(t;x_0),t) < 0$ for long times are those that are on, or asymptotic to, a uniformly finite-time hyperbolic trajectory, as our main theorem shows for flows with Eulerian time scales below Lagrangian time scales. The local unstable manifolds can be obtained from a backward-time calculation of $d_T(x_0)$. If needed, one can refine the first approximation produced by this algorithm by checking the remaining inequalities of Theorem 1. After this refinement, the simple algorithm we sketched above becomes a rigorous, computer-

assisted analytical criterion. In the numerical example treated in this paper such a refinement is not necessary, but in our current numerical experiments on two-dimensional turbulent velocity fields the refinement is important to implement (see Haller and Yuan[7]).

Once the uniformly hyperbolic invariant sets are located, one can compute their global stable manifolds gradually using, e.g., the straddling technique of You, Kostelich, and Yorke,[16] as implemented for discrete velocity fields by Miller *et al.*[10] This approach, therefore, enables one to build systematically a global geometric template for mixing, finding first the core structures, then developing their stable and unstable sets to the extent needed for transport calculations.

II. THE MAIN THEOREMS

Consider a two-dimensional velocity field

$$\dot{x}=u(x,t), \quad x\in\mathbb{R}^2, \tag{1}$$

where u is at least a class C^2 function of its variables. Assume that a solution $x(t)$ of this system is known. The Jacobian of the velocity field along a solution $x(t)$ is given by the time-dependent matrix $D_x u(x(t),t)$. We assume that on some finite time interval $[t_0,t_0+T]$, we have $\det D_x u(x(t),t)<0$, i.e., $D_x u(x(t),t)$ has real eigenvalues $-\lambda_1(t)<0<\lambda_2(t)$. [Since we did not assume incompressibility for $u(x,t)$, in general we have $\lambda_1\neq\lambda_2$.] We will need the quantities

$$\lambda_{k\,\min}=\min_{[t_0,t_0+T]}\lambda_k(t), \quad k=1,2, \tag{2}$$

which measure the minima of the norm of the eigenvalues. We also define the eigenvectors $e_1(t)$ and $e_2(t)$ corresponding to $-\lambda_1(t)$ and $\lambda_2(t)$, and we assume that they are normalized such $|e_k(t)|=1$ and are chosen such that $e_k(t)$ depends smoothly on t. We denote the angle between $e_1(t)$ and $e_2(t)$ by $\kappa(t)$ and note that $\sin\kappa(t)\neq 0$.

Throughout this paper, for matrices $A\in\mathbb{R}^{2\times 2}$, we shall use the notation $|A|=\sqrt{\Sigma_{i,j=1}^2|A_{ij}|^2}$. With this notation, the matrix of eigenvectors $M(t)=[e_1(t),e_2(t)]\in\mathbb{R}^{2\times 2}$ satisfies

$$|M|=\sqrt{2}, \quad |\det M|=|\sin\kappa(t)|. \tag{3}$$

We note that $M(t)$ is a differentiable function of t under our assumptions.

We now introduce the quantities

$$\alpha=\min_{t\in[t_0,t_0+T]}|\sin\kappa(t)|, \quad \beta=\max_{t\in[t_0,t_0+T]}|\dot{M}(t)|, \tag{4}$$

which are upper bounds on the norm of $M^{-1}/\sqrt{2}$ and $\dot{M}$, respectively. Finally, we define

$$\gamma=\frac{\sqrt{2}\beta[\alpha^2\lambda_{1\,\min}\lambda_{2\,\min}+\sqrt{2}\alpha\beta(\lambda_{1\,\min}+\lambda_{2\,\min})+2\beta^2]}{\alpha^3\lambda_{1\,\min}\lambda_{2\,\min}}. \tag{5}$$

In the following we will use the notion of *finite-time stable* and *unstable manifolds* for a given particle motion $x(t)$. By these manifolds we mean two-dimensional surfaces in the three-dimensional space of the (x,t) variables that contain motions asymptotic to $x(t)$. More precisely, a finite-time stable manifold for $x(t)$ on the time interval $[t_0,T]$ is a smooth, two-dimensional set of initial conditions (x_0,t_0) such that all the corresponding motions $x(t;t_0,x_0)$ approach $x(t)$ at a fixed exponential rate as long as $t\in[t_0,T]$. A similar definition applies for finite-time unstable manifolds (see Haller and Poje[6] for more details).

Our first main result, a set of sufficient criteria for hyperbolicity and uniform finite-time hyperbolicity, can now be stated as follows.

Theorem 1: *Suppose that for a solution $x(t)$ of (1) and for all $t\in[t_0,t_0+T]$,*

$$\det D_x u(x(t),t)<0, \quad \sqrt{2}\beta\left[\frac{1}{\lambda_{1\,\min}}+\frac{1}{\lambda_{2\,\min}}\right]<\alpha. \tag{6}$$

Then

(i) *$x(t)$ admits two-dimensional finite-time stable and unstable manifolds in the space (x,t) for $t\in[t_0,t_0+T]$.*

(ii) *If, in addition, for all $t\in[t_0,t_0+T]$*

$$\beta<\frac{\alpha}{2}\sqrt{2\lambda_{1\,\min}\lambda_{2\,\min}},$$

$$\lambda_1(t)>\gamma+\frac{2\beta^2}{\alpha^2\lambda_{1\,\min}\lambda_{2\,\min}}\lambda_2(t), \tag{7}$$

$$\lambda_2(t)>\gamma+\frac{2\beta^2}{\alpha^2\lambda_{1\,\min}\lambda_{2\,\min}}\lambda_1(t),$$

then $x(t)$ is uniformly finite-time hyperbolic on $[t_0,t_0+T]$.

Roughly speaking, our next result states that for flows where the rate of change of coherent structures stays below a critical limit, $\det D_x u(x(t),t)<0$ is also a necessary condition for $x(t)$ to be uniformly hyperbolic.

Theorem 2: *Suppose that a solution $x(t)$ of (1) is uniformly hyperbolic on the time interval $[t_0,t_0+T]$. Let $P(t)$ be a smooth matrix that contains unit vectors that are tangent to the $t=$const slice of finite-time stable and unstable manifolds of $x(t)$, and assume that*

$$|\det\dot{P}(t)||\det P(t)|+2\sqrt{2}|\dot{P}(t)||D_x u(x(t),t)| <|\det D_x u(x(t),t)||\det P(t)|^2. \tag{8}$$

Then we have $\det D_x u(x(t),t)<0$.

The proofs of Theorems 1 and 2 will be given in Sec. VI.

III. FINDING STABLE AND UNSTABLE MANIFOLDS IN APPLICATIONS

In this section we give some intuition for the conditions of Theorems 1 and 2. We also discuss sharper versions of the theorems as well as a numerical algorithm that locates candidates for uniformly hyperbolic trajectories.

A. Physical interpretation of Theorems 1 and 2

The conditions of Theorem 1 have the following meaning. The first inequality in Eq. (6) requires ''instantaneous hyperbolicity'' along the solution $x(t)$. This becomes transparent after one notes that along $x(t)$

$$DF_t^h(x(t)) = I + h\frac{d}{dh}DF_t^h(x(t))\big|_{h=0} + \mathcal{O}(h^2)$$

$$= I + hD_x u(x(t),t) + \mathcal{O}(h^2),$$

and hence if $-\lambda_1(t)$ and $\lambda_2(t)$ are the eigenvalues of $D_x u(x(t),t)$, then the eigenvalues of $DF_t^h(x(t))$ can be written as $1-h\lambda_1(t)+\mathcal{O}(h^2)$ and $1+h\lambda_2(t)+\mathcal{O}(h^2)$. The second condition in Eq. (6) ensures that the ''Eulerian'' time scales along $x(t)$ (measured by β) are sufficiently well separated from the Lagrangian time scales (measured by α). If the strength of instantaneous hyperbolicity (measured by $\lambda_{k\,\min}$) is stronger, then $(1/\lambda_{1\,\min})+(1/\lambda_{2\,\min})$ is a smaller quantity and hence the Eulerian and Lagrangian time scales are allowed to be closer to each other. Finally, the conditions in Eq. (7) require an even more pronounced separation of Eulerian and Lagrangian time scales along $x(t)$ in order to ensure uniform hyperbolicity.

While $\det D_x u(x(t),t)<0$ by itself is often used in fluid mechanics to identify hyperbolic regions in a flow (see, e.g., Weiss,[15] Elhmaïdi *et al.*,[4] and the references therein), the second condition in Eq. (6) is essential for $x(t)$ to be hyperbolic for the following reason. The linear stability of $x(t)$ on the time interval $[t_0,t_0+T]$ is determined by the stability of the origin in the variational equation

$$\dot{y} = D_x u(x(t),t)y.$$

In general, the stability of such a time-dependent linear system cannot be inferred from the eigenvalues of $D_x u(x(t),t)$ as numerous classic counterexamples show (see, e.g., Hale[5] or Verhulst[14]). However, all these counterexamples are based on the idea of introducing fast enough changes in the eigenvectors of $D_x u(x(t),t)$ as t increases, thereby destroying correlations between instantaneous hyperbolicity and actual stability in phase space along $x(t)$. In contrast, typical velocity fields in fluid mechanics do display a sufficient separation of Eulerian and Lagrangian time scales so that formulas (6) and (7) hold for uniformly hyperbolic sets.

All this is made rigorous by Theorem 2, which essentially says that in flows where coherent structures do not change very fast [i.e., the elements of the matrix $\dot{P}$ are small numbers compared to the product of the eigenvalues of $D_x u(x(t),t)$], a uniformly hyperbolic trajectory $x(t)$ will necessarily satisfy $\det D_x u(x(t),t))<0$. This second theorem is not meant to be a quantitative result as the estimates in its proof are far from being optimal. Rather, it serves as a theoretical underpinning for our numerical algorithm below. In particular, it guarantees that *strong enough uniformly hyperbolic sets can be found in typical fluid mechanical vector fields just by tracking the determinant of the Jacobian* $D_x u(x(t),t)$ *along particles*.

B. A sharper version of Theorem 1

Here we give an improvement of the conditions of Theorem 1. The improved conditions are somewhat more involved to implement numerically, yet they may give better results in given applications.

It can be seen from the inequality (21) in the proof of Theorem 1 that the second condition in Eq. (6) can be sharpened to

$$\max_{t\in[t_0,t_0+T]} \|M^{-1}(t)\| \max_{t\in[t_0,t_0+T]} \|\dot{M}(t)\| \left[\frac{1}{\lambda_{1\min}} + \frac{1}{\lambda_{2\min}}\right] < 1,$$

where $\|\cdot\|$ refers to the operator norm (i.e., for any $B \in \mathbb{R}^{2\times 2}$, $\|B\| = \sup_{|x|=1}(|Bx|/|x|)$ with $x\in\mathbb{R}^2$). In fact, the proof also reveals the even sharper condition

$$\max_{t\in[t_0,t_0+T]} \|M^{-1}(t)\dot{M}(t)\| \left[\frac{1}{\lambda_{1\,\min}} + \frac{1}{\lambda_{2\,\min}}\right] < 1.$$

C. The numerical algorithm

The statement of Theorem 1 gives a sufficient condition to locate uniformly finite-time hyperbolic trajectories. By Theorem 2, if the coherent structures in the velocity field do not change fast compared to particle speeds, the condition $\det D_x u(x(t),t)<0$ becomes necessary for $x(t)$ to be uniformly hyperbolic. This suggests the following simple procedure: 1. Consider a grid of initial conditions 2. Integrate each initial condition x_0 forward in time as long as $\det D_x u(x(t;x_0),t)$ is negative. 3. If $\det D_x u(x(t;x_0),t)<0$ for $t\in[t_0,t_0+T]$, then $x(t;x_0)$ is a candidate for a uniformly hyperbolic trajectory; check the remaining conditions of Theorem 2 to ascertain this.

The above ''naive'' algorithm would be very sensitive to numerical errors by the underlying instability of the uniformly hyperbolic sets that it intends to seek out. Indeed, the best one can hope for when one picks an arbitrary grid of initial conditions is to stay very close to the local stable manifold of a uniformly hyperbolic trajectory for a long time. For this reason, the following algorithm works significantly better in practice: 1. Consider a grid of initial conditions. 2. Integrate each initial condition x_0 forward in time as long as $\det D_x u(x(t;x_0),t)$ is negative. 3. Let $d_T(x_0)\in[0,T]$ denote the time for which $\det D_x u(x(t;x_0),t)$ stays negative [$d_T(x_0)=0$ will hold for initial conditions for which $\det D_x u(x(t_0;x_0),t_0)>0$]. 4. Local extrema of the scalar field $d_T(x_0)$ are candidates for the $t=t_0$ slices of local stable manifolds.

In principle, the above procedure should give the same result in forward and backward time. In practice, as is well known, local stable and unstable manifolds behave differently under numerical iterations. For this reason, performing the above algorithm first in forward time starting from $t=t_0$ will render $t=t_0$ slices of the local stable manifolds of uniformly hyperbolic sets, while iteration in backward time from $t=t_0$ will give the slices of local unstable manifolds. This is precisely the numerical scheme that we described in the Introduction. The intersection of the stable and unstable curves will clearly mark candidates for uniformly hyperbolic particle paths. For these, the remaining conditions of Theorem 1 may be verified. As we noted in Sec. I, in some examples this verification is crucial as the set of particles with long initial residence times in hyperbolic regions is too large. In other examples, such as the one described in Sec. IV be-

low, the emerging template of local stable and unstable manifolds is sharp enough so that further computations are not necessary.

While for analytically given vector fields the calculation of the Jacobian $D_x u(x(t),t)$ along the solution $x(t)$ is straightforward numerically, for experimentally or numerically defined velocity fields it needs to be interpolated. However, as opposed to the difficulties arising with similar calculations for finite-time Lyapunov exponents, here the results will be fairly robust and independent of the discretization scheme used. The reason is that one does not need to solve the variational equation associated with $D_x u(x(t),t)$, or compute higher powers of this matrix. In our numerical experiments for analytically given flows (see below), the field $d_T(x_0)$ showed no noticeable difference when first the exact Jacobian was used and then its approximation by finite differences.

IV. EXAMPLES

In this section we consider two examples that illustrate the use of Theorem 1. We start with a simple integrable example in which the outcome of a numerical experiment can be predicted without actually performing it. We then consider a nonintegrable example and test our algorithm along with another technique, the finite strain method (cf. Sec. I).

Example 1: (Duffing equation in a moving frame) Let us consider the time-dependent system

$$\dot{x}=u(x,t), \quad u(x,t)=\begin{pmatrix} x_2+(v_2-v_1)t \\ x_1+(v_1-v_2)t-(x_1+v_1 t)^3 \end{pmatrix}, \tag{9}$$

which is obtained by letting $x=y-vt$ with $v=(v_1,v_2)$ in the Duffing equation

$$\dot{y}_1=y_2, \quad \dot{y}_2=y_1-y_1^3. \tag{10}$$

We know that the only uniformly hyperbolic trajectory of Eq. (10) is the $y=0$ equilibrium as well as solutions in its local stable and unstable manifolds. We would like to see whether the sufficient criterion we gave in the previous section picks out $x=-vt$ and its local stable and unstable manifolds as uniformly hyperbolic sets for system (9).

On any solution $x(t)$ of Eq. (9) we have

$$D_x u(x(t),t)=\begin{pmatrix} 0 & 1 \\ 1-3(x_1(t)+v_1 t)^2 & 0 \end{pmatrix},$$

so we have $\det D_x u(x(t),t)<0$ if

$$|x_1(t)+v_1 t|<\frac{1}{\sqrt{3}}. \tag{11}$$

Thus, the first condition in Eq. (6) is satisfied for solutions of Eq. (9) which stay in a band of width $1/\sqrt{3}$ around the plane $x_1=v_1 t$ in the extended phase space of the variables (x_1,x_2,t). We know from the geometry of the Duffing equation [Eq. (10)] that for $t\in[t_0,t_0+T]$, the solutions satisfying Eq. (11) form an open neighborhood of the local stable and unstable manifolds of the solution $x=-vt$. This neighborhood is getting thinner and thinner as T increases. Therefore, for large enough T a numerical evaluation of the first condition in Eq. (6) would yield precisely the pieces of the local stable and unstable manifolds of $x=-vt$.

As for the second condition in Eq. (6), we note that on the solution $x=-vt$ we have

$$D_x u(-vt,t)=\begin{pmatrix} 0 & 1 \\ 1 & 0 \end{pmatrix},$$

therefore, on this solution

$$\det D_x u(-vt,t)=-1, \quad \alpha=\sqrt{2}, \quad \beta=0,$$

$$\gamma=0, \quad \lambda_{1\,\min}=\lambda_{2\,\min}=1.$$

Consequently, conditions (6) and (7) are satisfied for $x=-vt$ for all times, implying that it is a uniformly hyperbolic solution on any finite time interval. By continuity, close enough solutions in its local stable and unstable manifolds will also satisfy Eqs. (6) and (7).

We conclude that in this example our Jacobian algorithm picks out thin stripes around the stable and unstable manifolds around the local stable and unstable manifolds of $x=-vt$. The stripes shrink down to the local stable and unstable manifolds exponentially fast in T, and hence the results refine quickly in time. The verification of Eqs. (6) and (7) is not necessary since they are automatically satisfied.

Example 2: (Forced Duffing equation in a rotating frame). We now apply the change of coordinates

$$x=A(t)y=\begin{pmatrix} \cos\omega t & -\sin\omega t \\ \sin\omega t & \cos\omega t \end{pmatrix} y$$

to the Duffing equation [Eq. (10)] to obtain the system

$$\dot{x}=B(t)x-\begin{pmatrix} \sin\omega t(x_1\cos\omega t-x_2\sin\omega t)^3 \\ \cos\omega t(x_1\cos\omega t-x_2\sin\omega t)^3 \end{pmatrix},$$

where

$$B(t)=\begin{pmatrix} \sin 2\omega t & \omega+\cos 2\omega t \\ -\omega+\cos 2\omega t & -\sin 2\omega t \end{pmatrix}.$$

To break integrability, we add an $\mathcal{O}(1)$ periodic forcing term and consider the modified system

$$\dot{x}=B(t)x-\begin{pmatrix} \sin\omega t(x_1\cos\omega t-x_2\sin\omega t)^3 \\ \cos\omega t(x_1\cos\omega t-x_2\sin\omega t)^3 \end{pmatrix}+\begin{pmatrix} 0 \\ \sin\omega t \end{pmatrix}. \tag{12}$$

Without the sinusoidal forcing term, this time-dependent system would admit two homoclinic manifolds asymptotic to the $x=0$ equilibrium. The homoclinic solutions would differ from the usual pair of homoclinic solutions of the Duffing equation by a rotating component. Adding the forcing term is expected to break the homoclinic structures and perturb the origin into a hyperbolic periodic orbit. The location or even the existence of this hyperbolic trajectory is not obvious since the perturbation is large, and hence standard persistence results from dynamical systems do not apply.

We now use the Jacobian algorithm described in the previous section to locate uniformly hyperbolic trajectories in the above problem. We select the rotation speed $|\omega|<1$ in our experiments in order to push our method to its limits. This means that the coherent structures in the flow rotate at

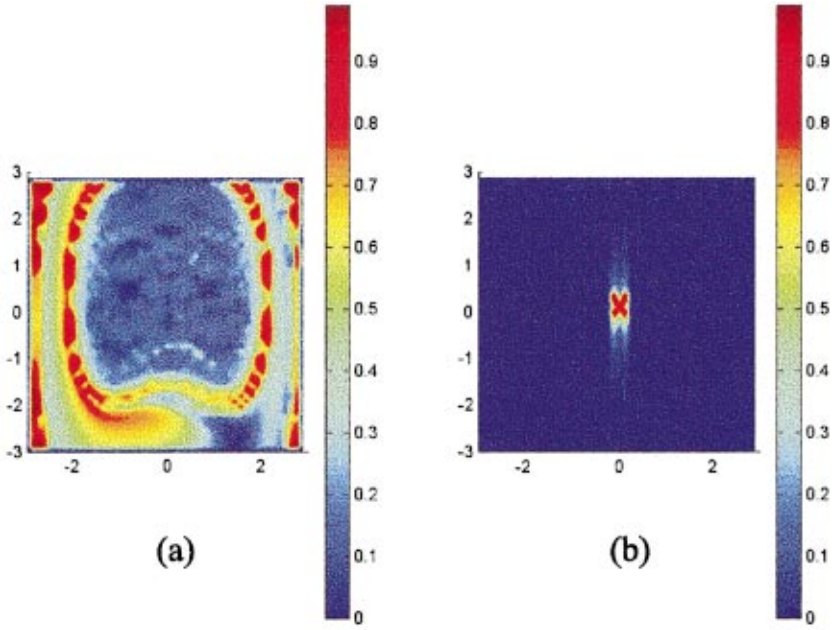

FIG. 2. (Color) Two different algorithms applied to the forced Duffing equation in a rotating frame. The number of initial conditions is 2500, taken from the square $[-3,3]\times[-3,3]$. The time of integration is $[0,15]$ for the stable manifold and $[0,-15]$ for the unstable manifold. (a) Visualization by the finite strain map algorithm, with the maximal strain normalized to 1. (b) Visualization by the Jacobian algorithm, with the maximal time $d_T(x_0)$ normalized to 1.

speeds almost comparable to particle speeds near the origin. In real-life flows of fluid mechanics this will typically not be the case.

As a first exploratory step, we use the finite strain map technique (see the Introduction) as well as the Jacobian algorithm on the square $[-3,3]\times[-3,3]$ of initial conditions. The solutions are integrated in both cases on the time intervals $[0,15]$ and $[0,-15]$ to obtain approximations for the $t=0$ slices of stable and unstable manifolds, respectively. We show the results for Fig. 2. The finite strain map technique highlights global maxima of stretching, but misses the underlying uniformly hyperbolic trajectory that is ultimately responsible for all the mixing. As expected, the Jacobian algorithm described in Sec. III C highlights only the core of the mixing template, the $t=0$ slices of the local stable and unstable manifolds a uniformly hyperbolic trajectory.

Aided by the above picture, we now focus on the smaller window $[-1,1]\times[-1,1]$ of initial conditions. This will help the finite strain algorithm since in this window the maximum of the strain is closer to the strain near the uniformly hyperbolic point. Indeed, as seen in Fig. 3, the finite strain algorithm initially gives a good approximation for the core of the mixing temple. However, even before the end of two forcing periods (4π), it starts producing a fuzzy picture from which the location of the underlying hyperbolic point is hard to guess. At $t=15$ the picture becomes unhelpful due to the

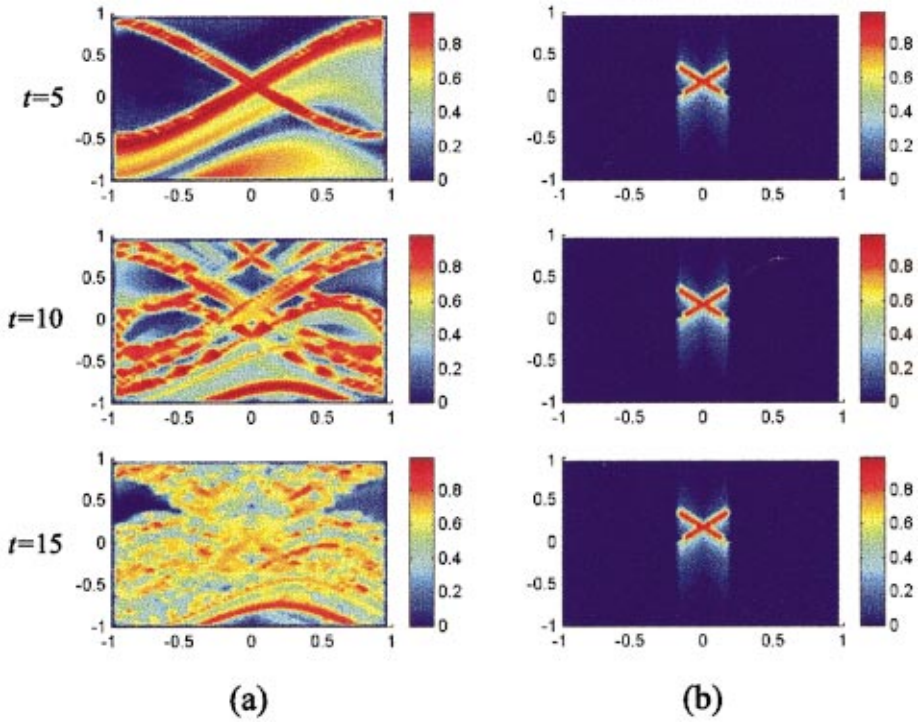

FIG. 3. (Color) Same as Fig. 2 for three different times of integration. The initial grid is the square $[-3,3]\times[-3,3]$ of 2500 particles. (a) Finite strain algorithm (b) Jacobian algorithm.

widespread strain near the homoclinic tangle. This is to be compared with the Jacobian calculation which consistently and sharply pinpoints the center of mixing. This illustrates the point we made earlier: The Jacobian algorithm is not sensitive to the choice of the time of integration; it only refines itself as t increases.

V. UNIFORM HYPERBOLICITY FOR FINITE TIMES

Here we give a precise definition for uniform finite-time hyperbolicity to set the stage for the proof of Theorems 1 and 2 in the next section. For the velocity field (1), the flow map $F_{t_0}^{\tau}: x_0 \mapsto x(t_0+\tau, x_0)$ associates the value of the solution $x(t,x_0)$ at time $t_0+\tau$ to its initial condition $x(t_0,x_0)\equiv x_0$. The linearized flow map along a solution $\varphi(t)$ can be written as

$$D_{t_0}^{\tau} = DF_{t_0}^{\tau}(\varphi(t_0)): \mathbb{R}^n \to \mathbb{R}^n. \tag{13}$$

Our main interest will be to describe uniform hyperbolicity for solutions on a time interval $[t_0, t_0+T]$, where $0<T<\infty$. With numerical applications in mind, our next definition of uniform finite-time hyperbolicity is motivated by similar definitions for discrete dynamical systems (see, e.g., Katok and Hasselblatt[8]).

Definition 1: *We call a solution* $\varphi(t)$ uniformly hyperbolic *on the time interval* $[t_0, t_0+T]$ *if for some constants* $0<\lambda$, $\mu<1$ *and for sufficiently small* $h>0$, *there exists a splitting* $\mathbb{R}^n = E_{\tau}^{+}(h) \oplus E_{\tau}^{-}(h)$ *depending continuously on* τ *and* h *such that*

$$D_t^h E_t^{\pm}(h) = E_{t+h}^{\pm}(h), \quad \|D_t^h|_{E_t^-(h)}\| \leqslant 1-h\lambda,$$

$$\|[D_t^h]^{-1}|_{E_{t+h}^+(h)}\| \leqslant 1-h\mu,$$

for all $t \in [t_0, t_0+T-h]$.

Roughly speaking, uniform hyperbolicity means that even arbitrarily short segments of the solution behave like ''saddles:'' They attract infinitesimally close initial conditions $x(\tau,x_0)$ along certain directions (i.e., along E_{τ}^{-}) and repel them along other directions (i.e., along E_{τ}^{+}). Uniformity is reflected by the fact that the constants λ and μ can be chosen independently of h and τ.

It is not hard to see that uniformly hyperbolic solutions are normally hyperbolic on any finite time interval $[t_0, t_0+T]$. Indeed, if for any $\tau \in (0,T]$ we let $h=\tau/N$ for a large enough positive integer N, then we obtain

$$\begin{aligned}\|D_{t_0}^{\tau}|_{E_t^-(h)}\| &= \|D_{t_0+T-h}^h D_{t_0+T-2h}^h \cdots D_{t_0+h}^h D_{t_0}^h|_{E_t^-}\| \\ &\leqslant \|D_{t_0+T-h}^h\| \|D_{t_0+T-2h}^h\| \cdots \|D_{t_0+h}^h\| \|D_{t_0}^h|_{E_t^-}\| \\ &\leqslant (1-h\lambda)^N = (1-h\lambda)^{\tau/h}.\end{aligned}$$

Since h can be arbitrarily small, we obtain

$$\|D_{t_0}^{\tau}|_{E_t^-(0)}\| \leqslant \lim_{h\to 0}(1-h\lambda)^{\tau/h} = e^{-\lambda\tau}, \quad \tau \in (0,T],$$

where the limit $\lim_{h\to 0} E_T^-(h) = E_t^-(0)$ exists by continuous dependence on h. A similar argument yields

$$\|D_T^{-\tau}|_{E_t^-(0)}\| \leqslant \lim_{h\to 0}(1-h\mu)^{\tau/h} = e^{-\mu\tau}, \quad \tau \in (0,T].$$

Therefore, uniformly hyperbolic solutions admit finite-time stable and unstable manifolds (see Haller and Poje[6]). As opposed to regular (infinite-time) invariant manifolds, finite-time stable and unstable manifolds are *not* unique. However, they are unique up to an error of $\mathcal{O}(e^{-cT})$ where $c>0$ is an appropriate constant. As a result, on long enough time intervals their nonuniqueness cannot be resolved numerically (cf. Haller and Poje[6]).

At the same time, hyperbolicity does not imply uniform hyperbolicity on the same time interval. For instance, solutions in the stable manifold of the hyperbolic fixed point of the ordinary pendulum are not uniformly hyperbolic on finite time intervals unless the initial condition x_0 is chosen close enough to the fixed point.

VI. PROOFS OF THE MAIN THEOREMS

A. Proof of Theorem 1

1. Setup

We start by introducing the change of coordinates $y=x-x(t)$, which puts Eq. (1) in the form

$$\dot{y} = D_x u(x(t),t)y + \mathcal{O}(|y|^2), \tag{14}$$

where $\mathcal{O}(|y|^2)$ terms do depend on t. Under the first condition in Eq. (6), for any $t \in [t_0, t_0+T]$ the matrix $D_x u(x(t),t)$ admits two real eigenvalues $-\lambda_1(t)<0<\lambda_2(t)$. We can then define the matrix $M(t)$ of eigenvectors as in Sec. III, and pass to a frame moving with the eigenvectors by letting $y=M(t)z$. The transformed system takes the form

$$\dot{z} = \Lambda(t)z + P(z,t) - Q(z,t), \tag{15}$$

with $\Lambda(t) = \mathrm{diag}(-\lambda_1(t), \lambda_2(t))$, $P(z,t) = \mathcal{O}(\|M^{-1}\||Mz|^2)$ and $Q(z,t) = M^{-1}\dot{M}z$. By Eq. (3), from the definitions of α and β from Eq. (4) we obtain

$$|P(z,t)| \leqslant \frac{2\sqrt{2}C}{\alpha}|z|^2, \quad |Q(z,t)| \leqslant \frac{\sqrt{2}\beta}{\alpha}|z|,$$

with an appropriate $C>0$ for $t \in [t_0, t_0+T]$. Note that in the z coordinates the original solution $x(t)$ satisfies $z\equiv 0$.

2. Integral equations

We fix two small constants $\delta, \Delta > 0$ and modify Eq. (15) in a C^{∞} fashion such that the modified vector field

$$\dot{z} = \tilde{\Lambda}(t)z + \tilde{P}(z,t) + \tilde{Q}(z,t), \tag{16}$$

is smooth for all $z \in \mathbb{R}^2$ and $t \in \mathbb{R}$, coincides with Eq. (15) for $|z_i| \leqslant \delta$ and $t \in [t_0+\Delta, t_0+T-\Delta]$, and obeys

$$\begin{aligned}&\tilde{\Lambda}_{11}(t) \leqslant -\lambda_{1\,\min} < 0 < \lambda_{2\,\min} \leqslant \tilde{\Lambda}_{22}(t), \\ &\tilde{\Lambda}_{12}(t) = \tilde{\Lambda}_{21}(t) \equiv 0, \quad t \in \mathbb{R}, \\ &|\tilde{P}(z,t)| \leqslant \delta\frac{2\sqrt{2}C}{\alpha}|z|, \quad |\tilde{Q}(z,t)| \leqslant \frac{\sqrt{2}\beta}{\alpha}|z|, \\ &\tilde{P}(z,t) = \tilde{Q}(z,t) \equiv 0, \quad t \notin [t_0, t_0+T], \quad \text{or} \quad |z| > 2\delta.\end{aligned} \tag{17}$$

(For more details of this construction we refer the reader to Haller and Poje[6]).

Introducing the notation

$$z=(z_s,z_u),\quad \tilde{P}=(\tilde{P}_s,\tilde{P}_u),\quad \tilde{Q}=(\tilde{Q}_s,\tilde{Q}_u),$$
$$\tilde{\lambda}_1=\tilde{\Lambda}_{11},\quad \tilde{\lambda}_2=\tilde{\Lambda}_{22},$$

then dropping the tildes, we obtain by integration from Eq. (16) the equations

$$\begin{aligned} z_s(t)&=e^{-\int_{t_s}^{t}\lambda_1(\tau)d\tau}z_s(t_s)+\int_{t_s}^{t}e^{-\int_{\tau}^{t}\lambda_1(s)ds}[P_s(z(\tau),\tau)\\ &\quad+Q_s(z(\tau),\tau)]d\tau,\\ z_u(t)&=e^{\int_{t_u}^{t}\lambda_2(\tau)d\tau}z_u(t_u)+\int_{t_u}^{t}e^{\int_{\tau}^{t}\lambda_2(s)ds}[P_u(z(\tau),\tau)\\ &\quad+Q_u(z(\tau),\tau)]d\tau. \end{aligned} \tag{18}$$

We want to construct a stable set W^s to the solution $z(t)\equiv 0$. The subset of this set falling in the interval $t\in[t_0+\Delta,t_0+T-\Delta]$ will serve as a finite-time stable set for the original solution $x(t)$. We define W^s as

$$W^s=\{z_0|\sup_{t\geqslant 0}|z(t;z_0)|<\infty\}.$$

In other words, W^s contains the set of initial conditions that remain bounded in forward time. W^s is a positively invariant set by definition, and for any solution $z(t)\in W^s$ and for any fixed $t\in\mathbb{R}$, we have

$$\lim_{t_u\to\infty}|e^{\int_{t_u}^{t}\lambda_2(\tau)d\tau}z_u(t_u)|\leqslant K\lim_{t_u\to\infty}e^{\int_{t_u}^{t}\lambda_2(\tau)d\tau}=0.$$

As a result, taking the limit $t_u\to\infty$ in Eq. (18), setting $t_s=0$ and $z_s(t_s)=z_s$, we obtain that solutions in W^s satisfy the integral equation

$$\begin{aligned} z_s(t)&=e^{-\int_0^t\lambda_1(\tau)d\tau}z_s+\int_0^t e^{-\int_{\tau}^{t}\lambda_1(s)ds}[P_s(z(\tau),\tau)\\ &\quad+Q_s(z(\tau),\tau)]d\tau,\\ z_u(t)&=\int_{\infty}^{t}e^{\int_{\tau}^{t}\lambda_2(s)ds}[P_u(z(\tau),\tau)+Q_u(z(\tau),\tau)]d\tau. \end{aligned} \tag{19}$$

We shall prove that this integral equation has a unique solution $z(t)$ with $z_s(0)=z_s$, which will imply that W^s is a nonempty set.

3. Normal hyperbolicity of $x(t)$

We rewrite Eq. (19) in the form

$$z(t)=\mathcal{F}(z(t)), \tag{20}$$

which shows that a solution of Eq. (19) is a fixed point of the map $\mathcal{F}$. We shall use the norm

$$\|z\|=\sup_{t\geqslant 0}|z(t)|$$

on the function space

$$B_K=\{z(t):[0,\infty)\to\mathbb{R}^2|z\in C^0[0,\infty),\ \|z\|\leqslant K\},$$

which is a complete metric space in the norm $\|\cdot\|$. We want to show that $\mathcal{F}$ is a contraction mapping on B_K in order to conclude the existence of a unique solution to Eq. (20).

First we show that $\mathcal{F}$ maps B_K into B_K. From the integral equation [Eq. (19)] and the estimates [Eq. (17)] we obtain

$$\begin{aligned} |\mathcal{F}(z(t))|&\leqslant e^{-\int_0^t\lambda_1(\tau)d\tau}|z_s|+\int_0^t e^{-\int_{\tau}^{t}\lambda_1(s)ds}[|P_s(z(\tau),\tau)|+|Q_s(z(\tau),\tau)|]d\tau+\int_t^{\infty}e^{\int_{\tau}^{t}\lambda_2(s)ds}[|P_u(z(\tau),\tau)|+|Q_u(z(\tau),\tau)|]d\tau\\ &\leqslant\delta e^{-\int_0^t\lambda_1(\tau)d\tau}+\left[\delta\frac{2\sqrt{2}C}{\alpha}+\frac{\sqrt{2}\beta}{\alpha}\right]\max_{t\in[t_0,t_0+T]}\int_0^t e^{-\int_{\tau}^{t}\lambda_1(s)ds}|z|d\tau\\ &\quad+\left[\delta\frac{2\sqrt{2}C}{\alpha}+\frac{\sqrt{2}\beta}{\alpha}\right]\max_{t\in[t_0,t_0+T]}\max_{t\in[t_0,t_0+T]}\int_t^{\infty}e^{\int_{\tau}^{t}\lambda_2(s)ds}|z|d\tau. \end{aligned} \tag{21}$$

if we let $|z_s|\leqslant\delta$. Taking the supremum of both sides over $t\geqslant 0$ and using $\|z\|\leqslant K$ gives

$$\|\mathcal{F}(z(t))\|\leqslant\delta+\left[\delta\frac{2\sqrt{2}C}{\alpha}+\frac{\sqrt{2}\beta}{\alpha}\right]\left(\frac{1}{\lambda_{1\,\min}}+\frac{1}{\lambda_{2\,\min}}\right)K.$$

This inequality shows that $\|\mathcal{F}(z(t))\|<K$ will hold if

$$\delta\left(\frac{2\sqrt{2}C}{\alpha}+\frac{1}{K}\right)\left(\frac{1}{\lambda_{1\,\min}}+\frac{1}{\lambda_{2\,\min}}\right)+\sqrt{2}\frac{\beta}{\alpha}\left(\frac{1}{\lambda_{1\,\min}}+\frac{1}{\lambda_{2\,\min}}\right)<1.$$

But this last inequality is always satisfied for $\delta>0$ small enough under the second assumption in Eq. (6).

We now want to argue that $\mathcal{F}$ is a contraction mapping on the space B_K. For any two functions $z,\hat{z}\in B_K$ with $z_s(0)=\hat{z}_s(0)$, the integral equation [Eq. (19)] holds, and an estimate similar to (21) gives

$$\|\mathcal{F}(z(t))-\mathcal{F}(\hat{z}(t))\|\leqslant\left(\delta\frac{2\sqrt{2}C}{\alpha}+\frac{\sqrt{2}\beta}{\alpha}\right)\left(\frac{1}{\lambda_{1\,\min}}+\frac{1}{\lambda_{2\,\min}}\right)\|z(t)-\hat{z}(t)\|.$$

Again, this inequality will hold for $\delta>0$ small under the second assumption in Eq. (6). We can, therefore, conclude

that Eq. (19) has a unique solution for any $|w_s|<\delta$ if δ is small enough. The derivative of the solution with respect to w_s obeys similar estimates; thus we obtain that the solution of Eq. (19) is a C^1 function of w^s, i.e., the set W^s is a C^1 manifold.

The existence of a C^1 manifold of solutions

$$W^u=\{z_0|\sup_{t\leqslant 0}|z(t;z_0)|<\infty\}$$

follows from a similar construction.

4. Uniform hyperbolicity of $x(t)$

In order to derive further conditions under which $x(t)$ becomes uniformly hyperbolic, we need a better understanding of the $\mathcal{O}(z)$ part of the integral equation [Eq. (19)]. This is equivalent to studying the system

$$\dot{z}=(\Lambda(t)+\overline{P}(z,t))z, \tag{22}$$

where for $t\in[t_0+\Delta,t_0+T-\Delta]$

$$\overline{P}(z,t)=\begin{cases} M^{-1}(t)\dot{M}(t) & |z|\leqslant\delta \\ 0 & |z|>2\delta \end{cases}.$$

For $t\notin[t_0+\Delta,t_0+T-\Delta]$, $\Lambda(t)$ and $\overline{P}(z,t)$ again denote the appropriately extended matrices used in Eq. (19). We also recall that

$$|\overline{P}(z,t)|\leqslant\frac{\sqrt{2}\beta}{\alpha}. \tag{23}$$

A contraction mapping argument identical to that in Sec. VI A 3 shows that under the second condition in Eq. (6), the $z\equiv 0$ solution of the system of ODE (ordinary differential equation) (22) admits two-dimensional stable and unstable manifolds, U^s and U^u. For $|z|\leqslant\delta$, the $t=$const slices of U^s and U^u are lines by the linearity of Eq. (22). Solutions in, say, U^s again satisfy the integral equation

$$z_u(t)=\int_{\infty}^{t}e^{\int_\tau^t\lambda_2(s)ds}\overline{P}_u(z(\tau),\tau)d\tau, \tag{24}$$

which gives the global bound

$$|z_u||_{U^s}<\frac{\sqrt{2}\beta\delta}{\alpha\lambda_{2\,\min}}, \tag{25}$$

after one uses the *a priori* estimate $|z|\leqslant\delta$ in Eq. (24). A similar argument leads to

$$|z_s||_{U^u}<\frac{\sqrt{2}\beta\delta}{\alpha\lambda_{1\,\min}}. \tag{26}$$

We now introduce a time-dependent linear change of coordinates along $z\equiv 0$ that will transform the manifolds U^s and U^u into orthogonal planes. Such a change of coordinates can be chosen as $z=S(z,t)w$ with

$$S(z,t)=\begin{pmatrix} 1 & e_2(t) \\ e_1(t) & 1 \end{pmatrix},\quad |z|\leqslant\delta.$$

The functions $e_i(t)$ obey the estimates

$$|e_1(t)|\leqslant\frac{\sqrt{2}\beta}{\alpha\lambda_{1\,\min}},\quad |e_2(t)|\leqslant\frac{\sqrt{2}\beta}{\alpha\lambda_{2\,\min}}. \tag{27}$$

This follows from the inequalities (25) and (26) and the linearity of $t=$const slices of U^s and U^u for $|z|\leqslant\delta$. In the w coordinates (22) becomes

$$\dot{w}=C(w,t)w \tag{28}$$

with

$$C(w,t)=S^{-1}(z,t)(\Lambda(t)+\overline{P}(z,t))S(z,t)-S^{-1}(z,t)\dot{S}(z,t).$$

Note that $C(w,t)$ is a diagonal matrix by construction. As a next step in our construction, we will estimate the signs of the diagonal elements of $C(w,t)$ for small enough w. We first note that for $|S(z,t)w|\leqslant\delta$

$$\|\dot{S}(z,t)\|=\mathcal{O}(\delta),$$

as one concludes by differentiating the integral equation [Eq. (24)], as well as the analogous equation for solutions on U^u. Since $S^{-1}(z,t)$ is uniformly bounded, a direct calculation gives the following expression for the first diagonal element of $C(w,t)$:

$$C_{11}=\frac{-\lambda_1+\overline{P}_{11}+e_1\overline{P}_{12}-e_2\overline{P}_{21}-e_1e_2(\lambda_2+\overline{P}_{22})}{1-e_1e_2}+\mathcal{O}(\delta). \tag{29}$$

Using the estimates (25) and (26) together with the first inequality in condition (7), we conclude that $1-e_1e_2>0$. As a result, the sign of C_{11} is determined by the sign of the numerator in Eq. (29). If

$$-\lambda_1+|\overline{P}_{11}|+|e_1||\overline{P}_{12}|+|e_2||\overline{P}_{21}|+|e_1||e_2|(\lambda_2+|\overline{P}_{22}|)<0, \tag{30}$$

then we can select δ small enough so that $C_{11}(w,t)<0$. Now Eqs. (23) and (27) together show that Eq. (30) holds if

$$\lambda_1-\frac{2\beta^2}{\alpha^2\lambda_{1\,\min}\lambda_{2\,\min}}\lambda_2>\gamma,$$

with γ defined in Eq. (5). But this last inequality is satisfied by the second assumption in condition (7) of Theorem 1, therefore, we conclude that $C_{11}(w,t)<0$ for $|S(z,t)w|\leqslant\delta$ and δ small enough. A similar argument shows that $C_{11}(w,t)>0$ holds for $|S(z,t)w|\leqslant\delta$ and δ small enough by the third assumption in condition (7).

With all this knowledge about system (28), we rewrite the full set of ODEs [equivalent to the integral equation (19)] in the w coordinates to obtain

$$\dot{w}=C(w,t)w+\mathcal{O}(|w|^2).$$

In this coordinate system the variational equation along the solution $w\equiv 0$ is of the form

$$\dot{\zeta}=C(0,t)\zeta,$$

where we used the fact that C has no explicit w dependence for w sufficiently small. The fundamental matrix solution $\Phi(t+h)$ with $\Phi(t)=I$ of this system is just the representa-

tion on the linearized flow map $D_t^h \equiv DF_t^h(u(t))$ of the original velocity field (1). Consequently, in the w coordinates we can write

$$D_t^h = I + hC(0,t) + \mathcal{O}(h^2).$$

For any $h>0$, the splitting $\mathbb{R}^n = E_t^+(h) \oplus E_t^-(h)$ with

$$E_t^-(h) = \{w | w_2 = 0\}, \quad E_t^+(h) = \{w | w_1 = 0\},$$

is invariant under the linearized flow, i.e., $D_t^h E_t^{\pm}(h) = E_{t+h}^{\pm}(h)$. Furthermore,

$$\|D_t^h|_{E_t^-(h)}\| = 1 + C_{11}(0,t)h + \mathcal{O}(h^2),$$

$$\|[D_t^h]^{-1}|_{E_{t+h}^+(h)}\| = 1 - C_{22}(0,t)h + \mathcal{O}(h^2),$$

for all $t \in [t_0, t_0+T-h]$. Since both $C_{11}(0,t)<0$ and $C_{22}(0,t)>0$, the solution $x(t)$ is uniformly hyperbolic by Definition 1 with the choice

$$\lambda = \min_{t\in[t_0,t_0+T]} \frac{|C_{11}(0,t)|}{2}, \quad \mu = \min_{t\in[t_0,t_0+T]} \frac{C_{22}(0,t)}{2}.$$

B. Proof of Theorem 2

Since $x(t)$ is assumed to be uniformly hyperbolic on $[t_0, t_0+T]$, for any fixed t in this interval the matrix $P(t)$ described in the statement of the theorem is defined. Applying the change of coordinates $y = P(t)z$ to the transformed equation [Eq. (14)] then gives

$$\dot{z} = \Lambda(t)z + \mathcal{O}(|z|^2),$$

where

$$\Lambda(t) = P^{-1}(t) D_x u(x(t),t) P(t) + P^{-1}(t)\dot{P}(t) = \begin{pmatrix} -\nu_1(t) & 0 \\ 0 & \nu_2(t) \end{pmatrix},$$

with $\nu_1(t), \nu_2(t) > 0$. (As in our earlier calculations, the $\mathcal{O}(|z|^2)$ terms have a general, explicit time-dependence.) Consequently, we must have

$$\det[E(t)+F(t)] < 0, \tag{31}$$

where

$$E(t) = P^{-1}(t) D_x u(x(t),t) P(t), \quad F(t) = P^{-1}(t)\dot{P}(t).$$

Now, a direct calculation shows that

$$\begin{aligned}
&\det[E(t)+F(t)] \\
&= \det E(t) + \det F(t) + \sum_{i\neq j} [E_{ii}(t)F_{jj}(t) - E_{ij}(t)F_{ji}(t)] \\
&\geqslant \det E(t) - |\det F(t)| - |\det F(t)||E(t)F^{-1}(t)| \\
&\geqslant \det[D_x u(x(t),t)] - \frac{|\det \dot{P}(t)|}{|\det P(t)|} - \frac{|\det \dot{P}(t)|}{|\det P(t)|} \times |E(t)||F^{-1}(t)| \\
&\geqslant \det[D_x u(x(t),t)] - \frac{|\det \dot{P}(t)|}{|\det P(t)|} - \frac{2\sqrt{2}}{|\det P(t)|^2} \times |\dot{P}(t)||D_x u(x(t),t)|,
\end{aligned} \tag{32}$$

where we used the fact that $|P(t)| = \sqrt{2}$ by assumption. Then, combining Eq. (31) with Eq. (32) and with assumption (8) of Theorem 2, we obtain that $\det[D_x u(x(t),t)] < 0$ must hold.

ACKNOWLEDGMENTS

I would like to thank Ken Bowman, Chris Jones, Pat Miller, Konstantin Mischaikow, Andrew Poje, and Sean Winkler for stimulating conversations and insights. This research was partially supported by NSF Grant No. DMS-98-00922, ONR Grant No. N00014-93-I-0691, and an Alfred P. Sloan Fellowship.

[1] H. D. I. Abarbanel, *Analysis of Observed Chaotic Data* (Springer-Verlag, New York, 1996).
[2] K. P. Bowman, ''Manifold geometry and mixing in observed atmospheric flows,'' preprint (1999).
[3] K. P. Bowman, ''Manifold geometry, mixing, and mixing barriers in the stratosphere,'' Nature (London) (to be published).
[4] D. Elhmaïdi, A. Provenzale, and A. Babiano, ''Elementary topology of two-dimensional turbulence from a Lagrangian viewpoint and single-particle dispersion,'' J. Fluid Mech. **257**, 533–558 (1993).
[5] J. K. Hale, *Ordinary Differential Equations* (Wiley-Interscience, New York, 1969).
[6] G. Haller and A. C. Poje, ''Finite-time transport in aperiodic flows,'' Physica D **119**, 352–380 (1998).
[7] G. Haller and G. Yuan, Hyperbolicity, mixing, and the Weiss criterion in two-dimensional turbulence (in preparation).
[8] A. Katok and B. Hasselblatt, *Introduction to the Modern Theory of Dynamical Systems* (Cambridge University Press, Cambridge, 1995).
[9] I. Mezić and S. Wiggins, ''A method for visualization of invariant sets of dynamical systems based on the ergodic partition,'' Chaos **9**, 213–218 (1999).
[10] P. D. Miller, C. K. R. T. Jones, A. M. Rogerson, and L. J. Pratt, ''Quantifying transport in numerically generated velocity fields,'' Physica D **110**, 105–122 (1997).
[11] K. Mischaikow, M. Mrozek, J. Reiss, and A. Szmyczak, ''Construction of symbolic dynamics from experimental times series,'' preprint (1999).
[12] A. C. Poje and G. Haller, ''Geometry of cross-stream mixing in a double-gyre ocean model,'' J. Phys. Oceanogr. **8**, 1649–1665 (1999).
[13] A. C. Poje, G. Haller, and I. Mezić, ''The geometry and statistics of mixing in aperiodic flows,'' Phys. Fluids A **11**, 2963–2968 (1999).
[14] V. Verhulst, *Nonlinear Differential Equations and Dynamical Systems* (Springer-Verlag, Berlin, 1990).
[15] J. Weiss, ''The dynamics of enstrophy transfer in 2-dimensional hydrodynamics,'' Physica D **48**, 273–294 (1991).
[16] Z. You, E. J. Kostelich, and J. A. Yorke, ''Calculating stable and unstable manifolds,'' Int. J. Bifurcation Chaos Appl. Sci. Eng. **1**, 605–624 (1991).